Available online at www.sciencedirect.com
SCIENCE DIRECT®
Journal of the European Ceramic Society 25 (2005) 2755–2758
www.elsevier.com/locate/jeurceramsoc

Development of surface phases in $Ba(Zn_{1/3}Nb_{2/3})O_3$–$Ba(Ga_{1/2}Ta_{1/2})O_3$ microwave dielectric ceramics

H. Hughes [a], F. Azough [a], R. Freer [a,*], D. Iddles [b]

[a] *Manchester Materials Science Centre, UMIST and University of Manchester, Manchester, M1 7HS, UK*
[b] *Filtronic Comtek, Ceramics Division, Enterprise Drive, Station Road, Four Ashes, Wolverhampton WV10 7DB, UK*

Available online 10 May 2005

Abstract

Ceramics in the system $Ba(Zn_{1/3}Nb_{2/3})O_3$–$Ba(Ga_{1/2}Ta_{1/2})O_3$ (BZN–BGT) were prepared by the mixed oxide route. Powders were calcined at 1200 °C for 4 h and sintered at temperatures in the range 1300–1450 °C. Products were characterized by scanning electron microscopy (SEM), X-ray diffraction (XRD) and wavelength dispersive spectroscopy (WDS) techniques.

During processing of the ceramics two secondary phases developed on the surfaces of the sintered ceramics as a result of Zn evaporation: $Ba_8Zn_1Ta_6O_{24}$ (816) and $Ba_4Nb_5O_{15}$ (BN). On the basis of this analysis, ceramics having the compositions of the two secondary phases were prepared independently by the mixed oxide route. Both ceramics have a hexagonal structure; the 816 phase has space group of *P*63*cm*.

Keywords: Perovskites; Niobates; Secondary phase; Dielectric properties

1. Introduction

Recent developments in wireless communication technology have increased the demand for low cost microwave components. Commercial microwave ceramics need to have specific selective parameters, which are high, unloaded Q value ($Q_u > 20{,}000$ at 2 GHz), high dielectric constant ($\varepsilon_r > 30$) and temperature coefficient of resonant frequency tunable through zero. $Ba(Zn_{1/3}Ta_{2/3})O_3$ is an important microwave dielectric, but attempts are being made to develop Nb_2O_5-based analogues due to the high cost of Ta_2O_5.

The influence of secondary, surface phases on the mechanical and dielectric properties of microwave dielectrics has been discussed by many authors.[1–4,6–8] Desu and O'Bryan[4] who first found the presence of the secondary surface phase on sintered BZT ceramics established the connection between the Zn volatilization, the presence of surface secondary phase and control of dielectric properties.

Later, Sumita et al.[8] found the hexagonal $Ba_5Nb_4O_{15}$ phase in Ba(Mg, Co, Nb)O_3 based dielectrics and suggested that the presence of this impurity phase has a negative effect on dielectric properties. Subsequently Tolmer and Desgardin[3] found a phase, believed to be $Ba_8Zn_1Ta_6O_{24}$, in BZT ceramics, but detailed experimental work showed the phase to be $BaTa_2O_6$. The presence of the $BaTa_2O_6$ secondary surface phase was discussed by Webb et al.[6] who related the presence of this phase to the high Q value in BZT materials.

In the present study, $Ba(Ga_{1/2}Ta_{1/2})O_3$ (BGT) was chosen as an end member of the solid solution, with BZN to improve the dielectric properties, particularly the Q value. The BZN–BGT compositions were prepared by the mixed oxide route. The development of secondary phases was investigated.

Previously the solid solution with BGT as an end member, with $Ba(Zn_{1/3}Ta_{2/3})O_3$ (BZT), was investigated by Kageyama,[9] who observed an improvement of the Q value with the addition of BGT. This paper focuses on microstructure development in BZT–BGT.

* Corresponding author. Tel.: +44 161 306 3564; fax: +44 161 200 8877.
E-mail address: Robert.Freer@manchester.ac.uk (R. Freer).

0955-2219/$ – see front matter © 2005 Published by Elsevier Ltd.
doi:10.1016/j.jeurceramsoc.2005.03.134

2. Experimental

2.1. Ceramic processing

$(1-x)$BZN–xBGT ($x = 0.0$–0.2) ceramics were prepared by the mixed oxide route. Standard electronic grade raw materials of purity >99.5% (with a mean particle diameter (d_{50}) ~1–3 μm) were batched in lots of 100–200 g for the various formulations. The powders were mixed in polypropylene bottles with 200 g of ZrO_2 milling media and 100 ml of deionized water for 16 h. Subsequently, they were dried at 80 °C, sieved and calcined at 1200 °C for 4 h. The powders were then re-milled for 8 h in deionized water containing 2 wt.% of PEG (MW 20,000) added as binder. After final drying and sieving the powders were pressed into discs of 20 mm diameter and sintered at temperatures in the range 1300–1450 °C for 2–16 h. All samples were sintered in high purity alumina crucibles. All ceramics had >97% theoretical density as determined by Archimedes water immersion technique.

2.2. Structural and microstructural characterization

Scanning electron microscopy (SEM) was performed on Philips XL30 FEG-SEM, operating at 8–20 kV. Secondary and backscattered images were recorded. Wavelength dispersive spectroscopy (WDS) was performed on a Cameca Electron probe microscope (model SX100), operating at 15 kV, to yield compositional information. For SEM and WDS analysis the samples were polished with diamond paste (6 μm and 1 μm) and with colloidal silica (OPS), and then carbon coated.

Conventional X-ray diffraction (XRD) analysis was performed on an APD Philips PW3710 with diffractometer operating at 50 kV and 40 mA. Scans were conducted with Cu Kα radiation with wavelength of 1.54056 Å in the range of 15–35° with a step size of 0.05°. The measurements were performed on the surface of the sintered pellets and on sectioned polished samples.

3. Results and discussion

3.1. Microstructures

Fig. 1 is a scanning electron micrograph of a BZN sample sintered at 1350 °C for 4 h. The image shows an equiaxed grain structure with grain sizes 5–10 μm. There is no visible presence of any secondary phase in the matrix. However, Fig. 2 (region near the edge of the BZN sample in Fig. 1) shows extensive secondary phases. The chemistry of the second phase was studied by WDS. The thickness of the secondary surface phases in the BZN samples is around 25 μm. It is believed that these secondary surface phases develop because of zinc volatilization.

Fig. 3 shows the presence of a secondary surface phases in a BZN ceramic doped with 20% BGT (denoted as BG20) sintered at 1350 °C for 4 h. For this composition, the thickness of the secondary surface phase region is about 50 μm, i.e. double the thickness in the end member of the BZN composition. An increasing amount of secondary surface phase was observed in the BZN–BGT compositions prepared with higher amounts of BGT.

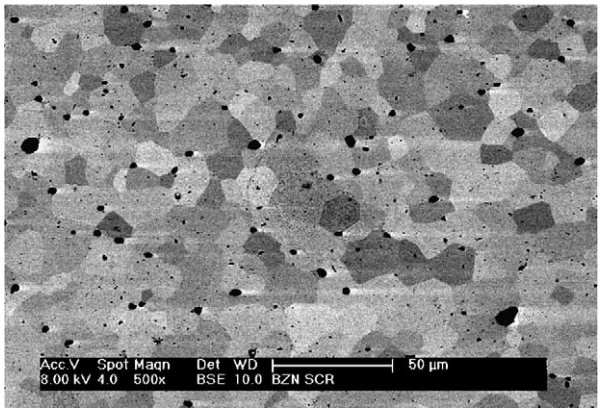

Fig. 1. SEM backscattered image of BZN specimen sintered at 1350 °C for 4 h.

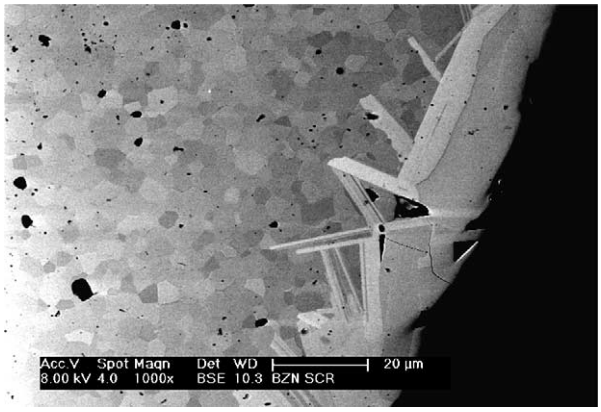

Fig. 2. SEM image of secondary surface phase in BZN specimen sintered at 1350 °C for 4 h.

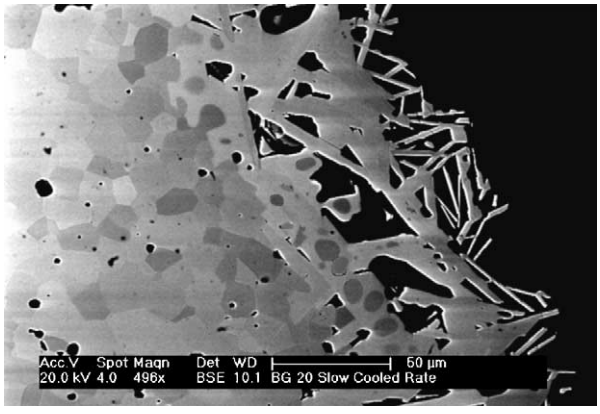

Fig. 3. SEM image of surface secondary phase for BG20 composition sintered at 1350 °C for 4 h.

The secondary, surface phases are formed as needle shaped particles. For the BZN composition, the needle shaped particles grows predominantly along the direction of the host ceramic grains. For compositions highly doped with BGT the needle shaped particles tend to grow towards the sintered surface.

The grain sizes were determined for all BZN–BGT compositions. It was noted that average grain size tended to increase with increasing amount of BGT in the initial formulation. The grain size for pure BZN is around 10 μm, but with increasing BGT the grain size increases to 18 μm in the BG20. Thus, additions of BGT to BZN increase the amount of secondary surface phase and the average grain size of the ceramic.

3.2. Chemical analysis

WDS analysis of the secondary surface phases showed the presence of two different secondary surface phases. At the outer edge of all samples the phase $Ba_5Nb_4O_{15}$ (BN) was found, i.e. all the Zn had evaporated. The thickness of this phase varies with compositions, but for BZN the thickness was around 15 μm. The remaining 10 μm of secondary surface phase was $Ba_8ZnNb_6O_{24}$ (816). The presence of this so-called 816 secondary surface phase is consistent with the findings of Davies et al.[1] and Bieringer et al.[2] for the BZT analogue system.

A detailed analysis of the BGT doped samples was undertaken to search for any additional phases, specifically Ta-rich and Ga-rich secondary phases. There was no evidence of any Ta-rich phase. However, a Ga-rich phase was found as part of the surface secondary phase. The Ga-rich phase formed as agglomerates, having a maximum size of 8 μm, in compositions highly doped with Ga (e.g. BG20). These agglomerates were distributed within the secondary surface phase of BZN–BGT compositions, mostly between the 816 and BN phases. By WDS this additional phase was established to be $Ba_3Ga_4O_9$. This Ga-rich phase is formed as a product of BGT doping. Very little is known about this phase, and it may be worthy of further investigation.

The importance of the presence of secondary surface phases on dielectric properties was previously discussed by Desu and O'Bryan[4] who found a positive influence of surface secondary phases on dielectric properties, particularly the *Q* value. They suggested that the reason for the increased *Q* value is lattice distortion. They proposed that Ba replaces the Zn on the B-site of the structure, and this will cause distortion, because the size of the Ba^{2+} ion is much larger than of Zn^{2+}.

The Zn volatilization and formation of the secondary surface phases in BZT ceramics was investigated by Davies et al.[1] The presence of so-called 816 phase was found on the tie line between pure BZT and $Ba_5Ta_4O_{15}$. The 816 phase exhibits very good dielectric properties and it was suggested to be a useful composition for microwave applications. Their finding for BZT ceramics is entirely consistent with the finding of this study, in which both 816 and BN phases were found in BZN-based ceramics.

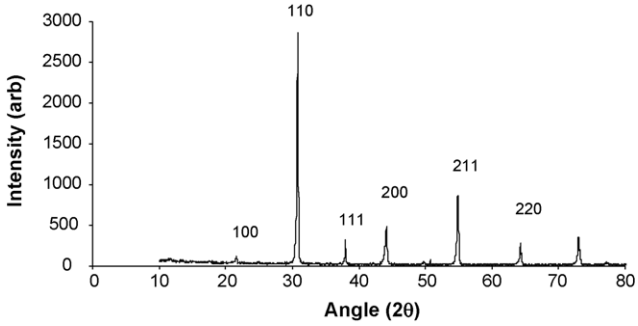

Fig. 4. X-ray diffraction spectrum for the matrix of BZN sample sintered at 1350 °C for 4 h.

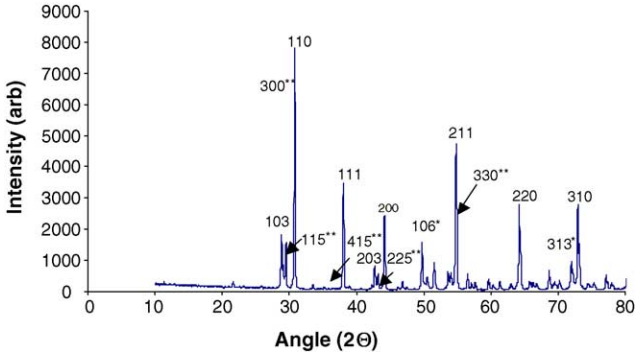

Fig. 5. X-ray diffraction spectrum for the sintered surface of BZN sample, sintered at 1350 °C for 4 h. The peaks '*' correspond to $Ba_5Nb_4O_{15}$; the peaks '**' correspond to $Ba_8Nb_6ZnO_{24}$.

3.3. Phase analysis

Fig. 4 shows an X-ray diffraction spectrum of the matrix of the end member BZN sintered at 1350 °C for 4 h. This spectrum confirms the perovskite structure without any evidence of a secondary phase.

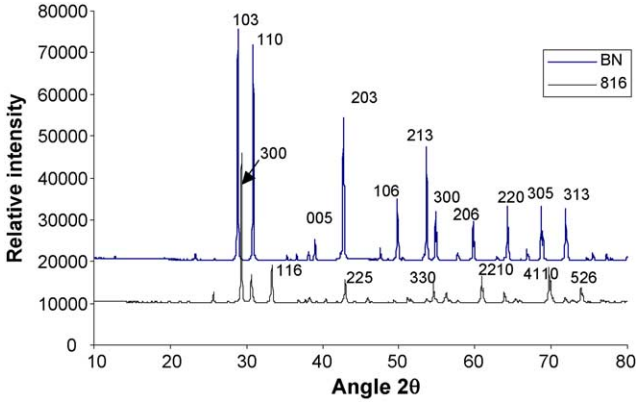

Fig. 6. X-ray diffraction spectra for specimens of $Ba_8Zn_1Nb_6O_{24}$ and $Ba_5Nb_4O_{15}$.

Fig. 5 is an X-ray diffraction spectrum for the surface of a sintered BZN specimen sintered at 1350 °C for 4 h. This spectrum shows the presence of secondary phases and confirmed that both $Ba_8ZnNb_6O_{24}$ and $Ba_5Nb_4O_{15}$ were present with the BZN matrix. For comparisons purposes, samples of the two secondary phases $Ba_5Nb_4O_{15}$ and $Ba_8ZnNb_6O_{24}$ were prepared and analysed. Fig. 6 shows XRD spectra for these two phases; they both exhibit the hexagonal structure;[1,2,5] the 816 phase has the space group *P*63*cm* and lattice parameters $a = 10.0643$ and $c = 19.006$. The BN composition has lattice parameters $a = 5.794$ and $c = 11.784$.

4. Conclusions

Two major secondary phases $Ba_5Nb_4O_{15}$ and $Ba_8ZnNb_6O_{24}$ were found on the surface of sintered BZN–BGT ceramics. The formation of these phases is due to Zn volatilization. The thickness of the secondary surface phases increases with an increasing amount of BGT in the starting mixture. Both secondary phases exhibit a hexagonal structure. A third Ga-rich minor phase ($Ba_3Ga_4O_9$) was found as part of the surface secondary phase, formed as a product of BGT doping.

References

1. Davies, P. K., Borisevich, A. and Thirumal, M., Communicating with wireless perovskites: cation order and zinc volatilisation. *J. Eur. Ceram. Soc.*, 2003, **23**, 2461–2466.
2. Bieringer, M., Moussa, S. M., Noailles, L. D., Burrows, A., Kiely, C. J., Rosseinsky, M. J., Ibberson, R. M. and Cation Ordering, Domain growth, and zinc loss in the microwave dielectric oxide $Ba_3ZnTa_2O_{9-\delta}$. *Chem. Mater.*, 2003, **15**(2), 586–597.
3. Tolmer, V. and Desgardin, G., Low-temperature sintering and influence of the process on the dielectric properties of $Ba(Zn_{1/3}Ta_{2/3})O_3$. *J. Am. Ceram. Soc.*, 1997, **80**(8), 1981–1991.
4. Desu, S. B. and O'Bryan, H. M., Microwave loss quality of $BaZn_{1/3}Ta_{2/3}O_3$. *J. Am. Ceram. Soc.*, 1985, **68**(10), 546–551.
5. Abakumov, A. M., Van Tendeloo, G., Scheglov, A. A., Shpanchenko, R. V. and Antipov, E. V., The crystal structure of $Ba_8Ta_6NiO_{24}$: cation ordering in hexagonal perovskites. *J. Solid State Chem.*, 1996, **125**, 102–107.
6. Webb, S. J., Scott, R. I., Cannell, D. S., Iddles, D. M. and Alford, N. M., Raman spectroscopic study of $Ba(Zn_{1/3}Nb_{2/3})O_3$. *J. Am. Ceram. Soc.*, 2002, **85**(7), 1753–1756.
7. Kim, D. W., Kwon, D. K., Hong, K. S. and Kim, D. J., Atmospheric dependence on dielectric loss of $16Ba_5Nb_4O_{15}{\cdot}56BaNb_2O_6$ ceramics. *J. Am. Ceram. Soc.*, 2003, **86**(5), 795–799.
8. Sumita, S., Kobayashi, M., Suzuki, K., Kawamura, K. and Miura, T., Microstrucure and microwave characteristics of $Ba\{(Mg,Co)_{1/3}Nb_{2/3}\}$-based dielectrics. *Jpn. J. Appl. Phys.*, 1991, **99**(8), 649–653.
9. Kageyama, K., Crystal structure and microwave dielectric properties of $Ba(Zn_{1/3}Ta_{2/3})O_3$–(Sr, Ba)$(Ga_{1/2}Ta_{1/2})O_3$ ceramics. *J. Am. Ceram. Soc.*, 1992, **75**, 1767–1771.